Critical and multicritical fluctuations of nematic liquid crystals

Z. H. Wang and P. H. Keyes
Department of Physics and Astronomy, Wayne State University, Detroit, Michigan 48202
(Received 22 July 1996)

The strong light scattering of a nematic liquid crystal is not necessarily only the result of director fluctuations. The director modes are just two of the five fluctuating modes of a nematic liquid crystal. The other three modes may also show strong scattering, comparable to or even larger than those of the director modes, in the vicinities of the certain critical and multicritical points obtainable in a nematic liquid crystal. We calculate in a unified approach and within a mean-field approximation the strength of the fluctuations of all five modes in a variety of circumstances, including critical, tricritical, and Landau multicritical points. Important information regarding these phase transitions can be learned by observing all five modes. [S1063-651X(96)12211-X]

PACS number(s): 61.30.Eb, 64.70.Md, 83.70.Jr

I. INTRODUCTION

The macroscopic order parameter associated with the orientational ordering of a liquid crystal is normally taken to be the anisotropic part of the dielectric tensor [1]. This tensor, being traceless and symmetric, has five independent components, all of which fluctuate about their equilibrium values at finite temperature. Usually, however, one focuses on the fluctuations of just two of these five components, the two transverse director modes. In the case of light scattering the contributions from the director fluctuations do indeed tend to dominate those of the other modes. However, there are well-known polarization rules for the light scattering from director modes that may be employed to block the director scattering and then allow one to observe the scattering from the other three modes. There is valuable information to be gained from the study of these other modes, particularly in the vicinity of phase transitions where they may exhibit pretransitional fluctuations comparable in magnitude to those of the director modes. Such transitions include, for example, changes in the type of orientational ordering as well as transitions from a nematic or even a chiral nematic liquid crystal to one of the various smectic phases.

This paper will present the results of calculations of the temperature dependences of the fluctuation strengths of all five modes at various transitions that involve changes in homogeneous orientational order only. We exclude from the present discussion, therefore, the very interesting but more complicated chiral nematic phases and blue phases, as well as all of the smectic phases. We will consider transitions from one type of nematic phase to another or from an isotropic phase to a nematic phase. There are several such transitions, related to the fact that there are nematic phases of three different types: uniaxial positive, uniaxial negative, and biaxial [1,2,3]. Associated with the various transitions are different types of critical or multicritical points. For example, there can be two lines of critical points separating the biaxial phase from the two types of uniaxial nematic phases with these lines merging and terminating at a special multicritical point also known as a Landau point [1,3,4]. Other types of critical points are found in the presence of an applied field; depending upon the sign of the coupling constant, one can have either an ordinary critical point [5–8] or else a tricritical point followed by a line of critical points [9].

The experimental realization of many of these critical or multicritical points has come about only fairly recently [4,10–12]. Likewise, the observation of critical opalescence within the nematic phase, as opposed to just within the isotropic phase, is fairly new [13,14]. It seemed timely, therefore, to undertake the systematic development of a theory of the fluctuations of a nematic liquid crystal in all these circumstances. In an earlier work it was shown how the light scattering could be calculated for two different geometries appropriate to a specific experiment [13]. Here we give the general methods of doing these calculations and apply them to the vicinities of all the above types of critical and multicritical points. Although we will make some comments on light scattering, our emphasis in this paper will be more on the zero-wave-vector limit of the critical phenomena.

The method we use is an application of the Landau–de Gennes free energy, which has already been so successful in describing the fluctuations of the five modes in the isotropic liquid on its approach toward the nematic phase [1,15,16]. We extend these calculations to include the fluctuations within the nematic phases, as well as the effects of external fields upon the fluctuations in both the isotropic and the nematic regions. In our approach the nematic order parameter is always treated as a five component object. The wide variety of critical phenomena displayed by nematic liquid crystals is in fact attributable to this multicomponent nature of the order parameter. One of the main advantages of the present approach is that it allows one to treat the fluctuations of the various modes on an equal footing and thus compare their relative importance.

The behaviors of the five different modes prove to be quite varied and interesting. For any given transition there are usually three different types of mode behavior. First of all, there will be at least one mode that ''goes critical,'' that is, one whose associated light scattering at $q=0$ diverges at the phase transition. From this divergence one extracts a critical exponent for a susceptibility (although in one important case we shall see that a different exponent is measured). Second, there will usually be one or more Goldstone modes, whose scattering at $q=0$ diverges not only at the phase transition, but throughout the entire condensed phase as well. An applied field can quench the fluctuations of such a mode, but,

as we shall see, this suppression is normally not very effective even for rather large fields. Third, from the remaining of the five modes, there will be one or more that are neither Goldstone nor critical modes and whose scattering does not diverge. Although one might suppose that the behavior of these modes are unremarkable, they often are just as interesting as the other modes, if not more so. Some show the most rapid changes of all the modes on the approach to a critical or multicritical point and provide the best means of locating such points. Others exhibit singular (but nondiverging) behavior at a critical point, allowing one to determine additional critical exponents, such as that of the coexistence curve.

In the next section we outline our methods and notation. The following several sections discuss individually the various types of critical and multicritical phase transitions that one finds in a nematic liquid crystal and the temperature dependences of their associated modes of fluctuation.

II. OUTLINE OF NOTATION AND METHODS

A. Notation

As is usual, we take our order parameter to be the anisotropic part of the dielectric tensor

$$Q_{\alpha\beta}=\epsilon_{\alpha\beta}-\tfrac{1}{3}\epsilon_{\gamma\gamma}\delta_{\alpha\beta}. \tag{1}$$

Light scattering takes place when this quantity fluctuates. Since $Q_{\alpha\beta}$ is both symmetric and traceless, it has just five independent components and can be written as [17]

$$Q_{\alpha\beta}=\frac{1}{\sqrt{6}}\begin{pmatrix}-Q & 0 & 0\\ 0 & -Q & 0\\ 0 & 0 & 2Q\end{pmatrix}+\frac{1}{\sqrt{2}}\begin{pmatrix}P_1 & P_2 & 0\\ P_2 & -P_1 & 0\\ 0 & 0 & 0\end{pmatrix}+\frac{1}{\sqrt{2}}\begin{pmatrix}0 & 0 & R_x\\ 0 & 0 & R_y\\ R_x & R_y & 0\end{pmatrix}. \tag{2}$$

The normalizations are chosen such that we have a simple form for the quadratic invariant

$$Q_{\alpha\beta}Q_{\beta\alpha}=Q^2+P_1^2+P_2^2+R_x^2+R_y^2, \tag{3}$$

where, as usual, repeated greek indices are summed over.

For the magnitudes of the five components of the order parameter we have used P, Q, and R with subscripts to distinguish the components that are qualitatively similar to each other. For a liquid crystal that is optically uniaxial with the optic axis oriented along the z direction, Q is the usual order parameter indicating the optical anisotropy and the P's and R's are zero on the average. Any fluctuations in Q about its average value describe changes in the *degree* of molecular ordering.

The P coefficients take on nonzero average values if the liquid crystal becomes optically biaxial. A biaxial nematic has another director field associated with a second symmetry-breaking direction. If this new director makes an angle ψ with respect to the x axis, then the P components are given by $P_1=P\cos2\psi$ and $P_2=P\sin2\psi$, where P is the *magnitude* of the biaxiality. P_1 is maximal and P_2 zero when the new symmetry direction lies along either the x or y axis. Variations of P_1 in this case would represent fluctuations in the degree of biaxiality, while changes in P_2 would be due to fluctuations of the new director. The roles of P_1 and P_2 are reversed if the symmetry-breaking direction is at 45° to the x or y axis; P_2 is then maximal, while P_1 is zero. For an arbitrary orientation of the new symmetry breaking direction, both P_1 and P_2 are nonzero. In this work we shall assume that $P\geqslant0$ and $\psi=0$, so that $P_1\geqslant0$ and $P_2=0$ on the average.

We use R's for the remaining two order parameter components partly to preserve alphabetical order, but also to remind us that they represent *rotations* of the uniaxial director. If this director should tilt slightly in the x direction, R_x will become nonzero to first order in the tilt angle and, similarly, R_y becomes nonzero for a tilt toward the y axis. (The P components will also become nonzero, but only to second order in the tilt.) Variations in the R's therefore represent director fluctuations. Some authors refer to the R and Q fluctuations as, respectively, ''transverse'' and ''longitudinal'' [18]. But since the P fluctuations also have transverse and longitudinal senses, we prefer not to use these designations.

Fluctuations in the above quantities are easily detected by light scattering. $I(\mathbf{q})$, the intensity of light with scattering wave vector $\mathbf{q}$, is proportional to $\langle|i_\alpha\delta\tilde{Q}_{\alpha\beta}(\mathbf{q})f_\beta|^2\rangle$, where $\delta\tilde{Q}_{\alpha\beta}(\mathbf{q})$ is the q transform of the $\alpha\beta$ component of the order parameter of Eq. (2) and i_α and f_β are, respectively, the polarization vectors of the incident and scattered light [1]. Thus, to see the mean-square fluctuations of R_x, the zx or xz component of $Q_{\alpha\beta}$, one should have $\hat{\mathbf{i}}$ oriented along z and $\hat{\mathbf{f}}$ along x or vice versa. A similar result holds for R_y, with y replacing x in the above. These geometries are the standard way of looking at director fluctuations: with one polarization vector parallel to the director and the other perpendicular. If both polarization vectors are parallel to the director one will see fluctuations in Q, the zz component of $Q_{\alpha\beta}$. Having $\hat{\mathbf{i}}$ oriented along x and $\hat{\mathbf{f}}$ along y or vice versa is the way to see fluctuations in P_2. The last two possibilities, having both polarizers oriented along the x direction or both along y, gives a mixed result. One then sees fluctuations in the square of $Q+P_1$ or of $Q-P_1$, respectively. If Q and P_1 are independent normal modes, as they are in many of the cases discussed below, then the average of the cross term is zero and one sees the average of $Q^2+P_1^2$ in both cases. One can then extract the average of P_1^2 if the Q fluctuations have been independently determined. If, however, Q and P_1 are *not* independent normal modes, the analysis is more complex.

B. Methods

To calculate the fluctuation effects we use the standard Landau–de Gennes free-energy density

$$\begin{aligned}\mathcal{F}=&\tfrac{1}{2}AQ_{\alpha\beta}Q_{\beta\alpha}+\tfrac{1}{2}L_1Q_{\alpha\beta,\gamma}Q_{\beta\alpha,\gamma}+\tfrac{1}{2}L_2Q_{\alpha\beta,\beta}Q_{\alpha\gamma,\gamma}\\&-\sqrt{\tfrac{2}{3}}BQ_{\alpha\beta}Q_{\beta\gamma}Q_{\gamma\alpha}+\tfrac{1}{4}C(Q_{\alpha\beta}Q_{\beta\alpha})^2\\&-\sqrt{\tfrac{3}{2}}\chi_aQ_{\alpha\beta}H_\alpha H_\beta.\end{aligned} \tag{4}$$

Here H_α is an external field (magnetic or electric) and χ_a is the anisotropic coupling constant associated with this field.

The choice of numerical coefficients has been made so as to simplify some of the ensuing equations. As usual, A is assumed to have a linear temperature dependence $A=A_0(T-T^*)$ and all the other coefficients are treated as constants. To obtain a more correct description of the temperature variation of the order parameter throughout a wide range of temperatures one should also assign temperature dependences to the B and C coefficients, but this refinement will not affect the nature of the critical behaviors that are the focus of the following sections and so will not be included. One important exception to the above, which will be discussed separately in Sec. VII, is the vicinity of the Landau multicritical point where the coefficient B changes sign.

In order to reduce the number of relevant parameters as much as possible, it is convenient to perform a scaling of variables such that $Q_{\alpha\beta}$ is measured in units of B/C, $\mathcal{F}$ in units of B^4/C^3, and $\chi_a H^2$ in units of B^3/C^2. This leads to the reduced expression

$$\mathcal{F}=\tfrac{1}{2}tQ_{\alpha\beta}Q_{\beta\alpha}+\tfrac{1}{2}l_1^2Q_{\alpha\beta,\gamma}Q_{\beta\alpha,\gamma}+\tfrac{1}{2}l_2^2Q_{\alpha\beta,\beta}Q_{\alpha\gamma,\gamma} - \sqrt{\tfrac{2}{3}}Q_{\alpha\beta}Q_{\beta\gamma}Q_{\gamma\alpha}+\tfrac{1}{4}(Q_{\alpha\beta}Q_{\beta\alpha})^2-\sqrt{\tfrac{3}{2}}\chi_a Q_{\alpha\beta}H_\alpha H_\beta. \tag{5}$$

In the above we have defined a reduced temperature $t\equiv AC/B^2$ and coherence lengths $l_{1,2}$, where $(l_{1,2})^2 \equiv L_{1,2}C/B^2$.

The standard method for computing the fluctuations in the isotropic phase in the absence of a field, where $Q_{\alpha\beta}$ is zero, is to retain only the quadratic terms of Eq. (5) and to apply the equipartition theorem to this harmonic approximation. In the nematic phase and/or in the presence of a field, where $Q_{\alpha\beta}$ is *not* zero, we likewise employ a harmonic approximation, although the procedure is somewhat more complex. First we must find $Q^{(0)}_{\alpha\beta}\equiv\langle Q_{\alpha\beta}\rangle$, the average value of $Q_{\alpha\beta}$, and then expand Eq. (5) out to second order in $\delta Q_{\alpha\beta}$, the deviations of $Q_{\alpha\beta}$ from this average. Thus we have

$$Q_{\alpha\beta}(\mathbf{r})=Q^{(0)}_{\alpha\beta}+\delta Q_{\alpha\beta}(\mathbf{r}) \tag{6}$$

and

$$\mathcal{F}(Q_{\alpha\beta}(\mathbf{r}))=\mathcal{F}(Q^{(0)}_{\alpha\beta})+\mathcal{F}_2(\delta Q_{\alpha\beta}(\mathbf{r})), \tag{7}$$

where $\mathcal{F}_2$ is second order in the $\delta Q_{\alpha\beta}$'s, all linear terms being absent since $\mathcal{F}$ evaluated at $Q^{(0)}_{\alpha\beta}$ is by definition a minimum with respect to variations of $\delta Q_{\alpha\beta}$. This procedure is indicated schematically in Fig. 1.

In order to find $Q^{(0)}_{\alpha\beta}$ we first substitute Eq. (2) into Eq. (5), omitting the gradient terms, to obtain

$$\mathcal{F}=\tfrac{1}{2}t(Q^2+P_1^2+P_2^2+R_x^2+R_y^2)-\tfrac{1}{3}Q^3+Q(P_1^2+P_2^2) -\tfrac{1}{2}Q(R_x^2+R_y^2)-\tfrac{\sqrt{3}}{2}P_1(R_x^2-R_y^2)-\sqrt{3}P_2R_xR_y +\tfrac{1}{4}(Q^2+P_1^2+P_2^2+R_x^2+R_y^2)^2-hQ, \tag{8}$$

and then we must find the Q, P's, and R's that minimize $\mathcal{F}$. Since the free energy is fully rotationally invariant, there will, in general, be an infinite number of solutions to this minimization problem corresponding to all the possible ways of orienting the coordinate axes with respect to the principle axes of the order parameter tensor. To simplify the analysis it will therefore be useful at the start to have the coordinate axes aligned with the principle axes as well as with any external fields so that as many components of order parameter as possible will be identically zero. For this reason, in deriving Eq. (8) above we have assumed that H_α is along the z direction, with the result that it only couples to the Q component. For further convenience we have also introduced a reduced field h defined by $h=\chi_a H^2$.

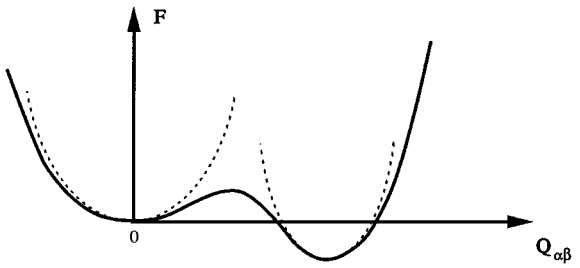

FIG. 1. Schematic of the free-energy surface at a temperature just below the first-order isotropic-nematic phase transition. The dotted lines are harmonic approximations to the two local minima, the higher left-hand one corresponding to a metastable isotropic phase at this temperature and the right-hand one to a thermodynamically stable nematic phase. The abscissa represents five coordinates, the independent components of the $Q_{\alpha\beta}$ order parameter tensor.

Next, to find $\mathcal{F}_2$, we put $Q^{(0)}_{\alpha\beta}$ back into Eq. (8) with the gradient terms restored and expand to second order in the $\delta Q_{\alpha\beta}$'s. Because of the gradient terms, it is easiest to find expressions for the average fluctuations of the Fourier transforms of the $\delta Q_{\alpha\beta}$'s, which are the quantities actually measured by light-scattering experiments.

In the next several sections we illustrate the application of these methods to the varieties of critical points mentioned in the Introduction. First, however, in Sec. III we study a more familiar case: the ordinary isotropic-nematic transition in the absence of any field. As it is well known, this transition is first order, but weakly so, and has some features resembling those of second-order transitions. It will be especially interesting to see how those features evolve toward full-fledged critical or multicritical behavior as we approach the various types of critical points discussed in Secs. IV–VII.

III. THE ISOTROPIC-NEMATIC TRANSITION

A. Review of the phase transition properties and "critical" exponents

For the uniaxial nematic aligned along the z axis (that is, with $P_1=P_2=R_x=R_y=0$) Eq. (8) reduces to the simpler and more familiar free-energy expression

$$\mathcal{F}=\tfrac{1}{2}tQ^2-\tfrac{1}{3}Q^3+\tfrac{1}{4}Q^4-hQ. \tag{9}$$

Before calculating the strengths of the fluctuations of the five modes, we first review and summarize the predictions stemming from the free-energy expression of Eq. (9), particularly for the field-free case. Although some of these results already appear several places in the literature, others do not to our

knowledge. Minimization of this equation gives the following cubic equation that must be solved to obtain Q_0, the equilibrium value of Q:

$$0 = tQ - Q^2 + Q^3 - h. \tag{10}$$

For the field-free case ($h=0$) there is a first-order phase transition at a temperature T_c, corresponding to a reduced temperature $t=\frac{2}{9}$, and the relevant solutions to Eq. (10) are

$$Q_0(t) = \begin{cases} 0, & t > \frac{2}{9} \quad \text{(11a)} \\ \frac{1}{2}(1+\sqrt{1-4t}), & t < \frac{2}{9}. \quad \text{(11b)} \end{cases}$$

The susceptibilities above and below this transition are given by

$$\frac{\partial Q}{\partial h}(t) = \begin{cases} \dfrac{1}{t}, & t > \frac{2}{9} \quad \text{(12a)} \\ \dfrac{2}{1-4t+\sqrt{1-4t}}, & t < \frac{2}{9}. \quad \text{(12b)} \end{cases}$$

The specific heat (in suitably reduced units) obtained from Eq. (9) is given by

$$C_h(t) = \begin{cases} 0, & t > \frac{2}{9} \quad \text{(13a)} \\ \dfrac{1}{2}\left(1 + \dfrac{1}{\sqrt{1-4t}}\right), & t < \frac{2}{9}. \quad \text{(13b)} \end{cases}$$

The mean-field predictions of Eqs. (11)–(13) contain singularities that imply a certain set of critical exponents for this transition. There is not critical behavior in the usual sense since the full singular behavior is interrupted by the first-order transition. Also related to this first-order character is the fact that the effective critical temperature, as well as the set of critical exponents, are different on the two sides of the phase transition.

We review first the behavior as seen from the isotropic side of the transition. From Eq. (12a), we see that the susceptibility diverges at $t=0$ or, to be more accurate, would diverge at this point if it were not interceded by a first-order transition at $t=\frac{2}{9}$ (i.e., $T=T_c$). Thus the effective critical temperature seen from above the transition is $t=0$ or, equivalently, $T=T^*$. Since the susceptibility diverges *linearly* as this point is approached, the mean-field prediction for the corresponding critical exponent is $\gamma=1$. This is probably the best known of the mean-field predictions and is followed quite accurately by nearly all measurements made to date. We also see from Eq. (12a) that $\alpha=0$ since there is no predicted divergence in the specific heat above T_c. (We do not consider here the inclusion of fluctuation effects that could produce an exponent $\alpha>0$, in better agreement with experiment.)

As seen from the nematic side of the transition, the susceptibility and the specific heat would diverge at $t=\frac{1}{4}$, according to Eqs. (12b) and (13b). The effective critical temperature, which we call T^{**}, is therefore closer to T_c ($t=\frac{2}{9}$) than is T^* ($t=0$) by a factor of 8. Nonetheless, because of the presence of ''background'' terms, it is harder to see the critical anomalies in the nematic than in the isotropic phase, where there is no such background. For example, the specific heat of Eq. (13b) has a constant plus an inverse square root divergence (implying a critical exponent of $\alpha'=\frac{1}{2}$). At the transition the singular part is only three times larger than the constant background. The situation is similar for the susceptibility. Equation (12b) has a linear plus a square-root divergence, the latter of which becomes the dominant singularity at T^{**} (implying a critical exponent of $\gamma=\frac{1}{2}$). But at the transition there is again this three-to-one ratio between these two contributions making it difficult to clearly discern the $\gamma=\frac{1}{2}$ exponent. Finally, from Eq. (11b) we see that the order parameter has a square-root dependence near T^{**}, corresponding to a critical exponent $\beta=\frac{1}{2}$. However, the order parameter does not go to zero at T^{**}, but to a finite or background value of $\frac{1}{2}$.

All in all, the critical behavior of this transition is unconventional to say the least. With the results quoted above it is clear that the scaling relations $\alpha+2\beta+\gamma=2$ and $\alpha'+2\beta+\gamma'=2$ are satisfied, but the hyperscaling equations $\alpha=\alpha'$ and $\gamma=\gamma'$ are not. Perhaps we should not expect any more of a first-order transition where, it could be argued, scaling ideas need not apply in the first case. However, as we have already stressed, this first-order transition can be brought through a variety of means to several different types of second-order transitions where scaling expectations *must* then hold. One of the things that will be interesting to see in the next several sections is how the unconventional behavior of this first-order transition evolves into the conventional as the various fields that produce true critical behavior are applied.

B. Calculation of the fluctuations

We return now to the calculation of the formulas for the fluctuations of the five modes, which, as we shall see, mimic the results of Eqs. (11)–(13) for the critical singularities. First we substitute Eq. (6) into Eq. (5) and keep terms up to second order in $\delta Q_{\alpha\beta}$. Then, as discussed previously, we switch to momentum representation by expressing the fluctuations of the order parameter in terms of its Fourier amplitudes

$$\delta Q_{\alpha\beta}(\mathbf{r}) = \sum_{\mathbf{q}} \widetilde{\delta Q}_{\alpha\beta}(\mathbf{q}) e^{i\mathbf{q}\cdot\mathbf{r}} + \text{c.c.} \tag{14}$$

Thus, for F_2, found by integrating the fluctuation part of the free-energy density over all space, viz., $F_2 = \int \mathcal{F}_2 d\mathbf{r}$, we obtain

$$\begin{aligned} F_2 = \sum_{\mathbf{q}} \{ & \tfrac{1}{2}(t - 2Q_0 + 3Q_0^2 + l_1^2 q^2) |\widetilde{\delta Q}(\mathbf{q})|^2 \\ & + \tfrac{1}{2}(t + 2Q_0 + Q_0^2 + l_1^2 q^2)[|\widetilde{\delta P_1}(\mathbf{q})|^2 + |\widetilde{\delta P_2}(\mathbf{q})|^2] \\ & + \tfrac{1}{2}(t - Q_0 + Q_0^2 + l_1^2 q^2)[|\widetilde{\delta R_x}(\mathbf{q})|^2 + |\widetilde{\delta R_y}(\mathbf{q})|^2] \}. \end{aligned} \tag{15}$$

It will be noticed in the above that we have dropped the contributions from the l_2 gradient term. In doing so we are making the so-called one-constant approximation, equivalent to assuming that the three Frank elastic constants, for splay,

bend, and twist, are equal to each other. [The expression of Eq. (4) is already somewhat approximate in that it has only two elastic constants.]

The motivation for eliminating the l_2 term, in addition to reducing the number of parameters in the theory, is that the presence of this term can make the calculation of the fluctuations in the nematic phase much more difficult. With the l_2 term retained there would be terms in Eq. (15) deriving from an expression $\frac{1}{2}l_2 q_\alpha Q_{\alpha\beta} Q_{\beta\gamma} q_\gamma$ in the Fourier-transformed free energy. If the scattering wave vector **q** is strictly in the z direction this gives $\frac{1}{4}l_2 q^2(\frac{4}{3}\tilde{Q}^2+\tilde{R}_x^2+\tilde{R}_y^2)$, a diagonal expression that causes no problems. If, however, the wave vector **q** makes an arbitrary angle with respect to the director, so that **q** and **n** each single out a specific spatial direction, terms involving cross products of the $\tilde{Q}$, $\tilde{P}$'s and $\tilde{R}$'s will appear in Eq. (15) and these quantities will no longer be normal modes. Although we can still calculate their mean-square fluctuations, the results are much more complex than when simple equipartion can be applied. In Sec. V B we in fact show how to deal with one of these cross terms, which cannot be avoided in that case since the director and the applied field are in different directions. But for the present we will avoid such complications since they tend to obscure the physical content of the results and do not, as far as we can tell, lead to any new interesting physics. In fact, all of our major results following this section will be given for the simplest case of the hydrodynamic or $q=0$ limit, where the gradient terms have no effect anyhow.

Now we use the solutions of Eq. (11) to evaluate the coefficients appearing in Eq. (15) and then the equipartition theorem to find the thermal averages of the fluctuations of the five modes. For $t>\frac{2}{9}$, the *isotropic phase*, we find

$$\langle|\widetilde{\delta Q}(\mathbf{q})|^2\rangle=\langle|\widetilde{\delta P_1}(\mathbf{q})|^2\rangle=\langle|\widetilde{\delta P_2}(\mathbf{q})|^2\rangle=\langle|\widetilde{\delta R_x}(\mathbf{q})|^2\rangle$$
$$=\langle|\widetilde{\delta R_y}(\mathbf{q})|^2\rangle=\frac{k_BT}{t+l_1^2q^2}, \tag{16}$$

while for $t<\frac{2}{9}$, the *nematic phase*, we obtain

$$\langle|\widetilde{\delta Q}(\mathbf{q})|^2\rangle=\frac{2k_BT}{1-4t+\sqrt{1-4t}+2l_1^2q^2}, \tag{17a}$$

$$\langle|\widetilde{\delta P_1}(\mathbf{q})|^2\rangle=\langle|\widetilde{\delta P_2}(\mathbf{q})|^2\rangle=\frac{2k_BT}{3(1+\sqrt{1-4t})+2l_1^2q^2}, \tag{17b}$$

$$\langle|\widetilde{\delta R_x}(\mathbf{q})|^2\rangle=\langle|\widetilde{\delta R_y}(\mathbf{q})|^2\rangle=\frac{k_BT}{l_1^2q^2}. \tag{17c}$$

The results for the isotropic phase are well known [15,16,19], but those for the nematic phase, to the best of our knowledge, are new and deserve comment.

First of all, we see that the two R modes within the nematic phase do indeed have the q^{-2} dependence expected for director fluctuations. The equation (10) that gives the equilibrium value of Q ensures that the coefficients of the R terms in Eq. (15) will vanish when $h=0$ except for the q^2 parts. This illustrates an important advantage of the approach we are using: by treating all five components of the order parameter on an equal footing and using a free-energy expression that is fully rotationally invariant, it is guaranteed that symmetry will be respected and that all those modes that should be Goldstone modes will be.

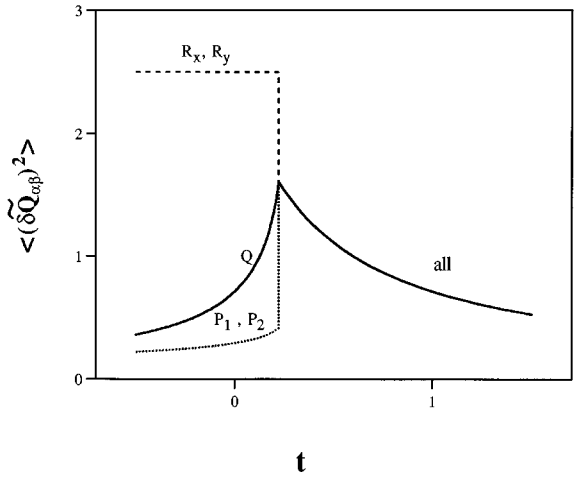

FIG. 2. Average square fluctuations of the order parameter components (in units of k_BT) at the ordinary nematic-isotropic transition, which occurs at a reduced temperature $t=\frac{2}{9}$. For this plot a value of $l_1^2q^2=0.4$ has been used.

The above equations reveal an interesting relationship between the isotropic scattering and that due to director fluctuations. The latter have the strength pretransitional critical scattering of the isotropic phase [Eq. (16)] would have if it could reach the effective critical point ($t=0$). Thus the large scattering exhibited by a nematic liquid crystal can in a sense be thought of as a type of critical opalescence that exists not just at the critical point but throughout the entire nematic phase. How large the director scattering is compared to the largest pretransitional scattering of the isotropic phase can be assessed by taking the ratio of Eq. (17c) to Eq. (16) evaluated at the transition temperature $t=\frac{2}{9}$. This ratio is, of course, dependent upon wavelength and scattering angle through q and is also material dependent through l_1. For thermotropic compounds l_1 is typically of the order of 100 Å and so for visible light scattered at about 90° the director scattering turns out to be about four times larger than the largest pretransitional scattering. In lyotropic systems it turns out that this ratio can be much closer to unity [13] and the two types of scattering may be comparable at the phase transition. In Fig. 2 we graph the results of Eqs. (16) and (17), measured in units of k_BT, using an arbitrarily chosen value for $l_1^2q^2$ of 0.4 that is roughly midway between typical thermotropic and lyotropic behaviors.

In Fig. 3 we plot the *inverse* of the expressions of Eqs. (16) and (17), measured in units of $1/k_BT$, versus the reduced temperature t. This corresponds to the most common way of representing light-scattering results and shows immediately the linear divergence of the scattered light in the isotropic phase. At the same time the negative curvature of the Q curve in the nematic phase shows clearly that the susceptibility exponent γ' is less than 1, as discussed earlier. The results in this figure are shown for the $q=0$ limit so that we can extrapolate the isotropic linear behavior to obtain T^* directly. For comparison purposes we will express all of our

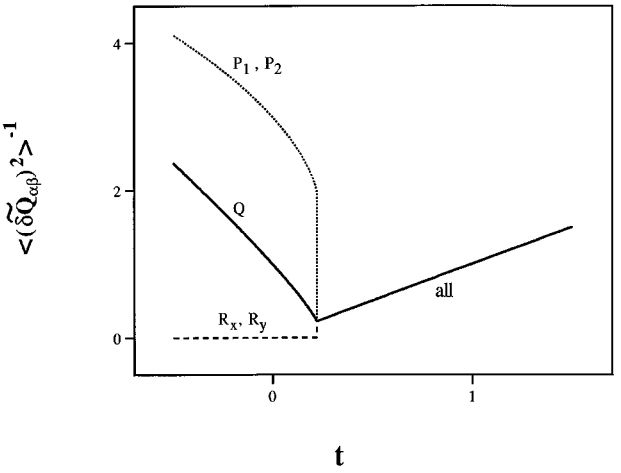

FIG. 3. Inverse of the average square fluctuations of the order parameter components in the vicinity of the ordinary nematic-isotropic transition. Here and in all the following figures showing fluctuations the $q=0$ limit is assumed and the ordinate is in units of $1/k_BT$.

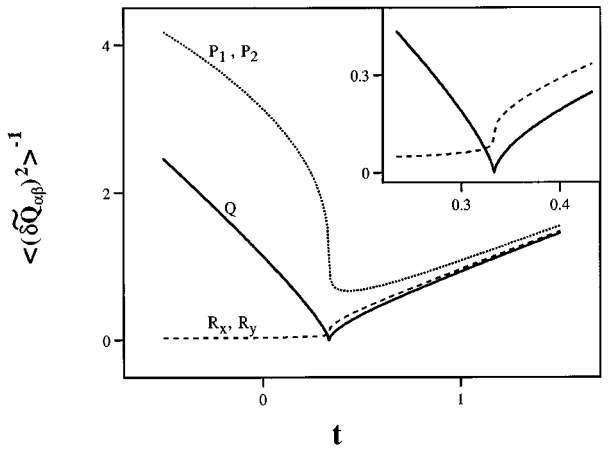

FIG. 4. Inverse of the average square fluctuations of the order parameter components for $q=0$ in the vicinity of the field-induced nematic-paranematic critical point. The critical point is at $t=\frac{1}{3}$ and $h=\frac{1}{27}$. Inset: enlargement of the critical region.

results from now on in this $q=0$ limit. Then, in the cases where the transition is second order, we will see that at least one of these curves, associated with a diverging susceptibility, will go to zero. Furthermore, any true Goldstone modes, such as the R modes in this case, will be represented by curves having zero value throughout the symmetry-broken phase.

The degeneracy of the five modes in the isotropic phase as seen in Fig. 3 would be removed somewhat if we had retained the l_2 gradient term and assume a value of $q\neq 0$. There would then be a slight splitting, with the two P modes fluctuating the most (least) for $l_2>0$ (<0) and the Q mode the least (most). There would be no other obvious effects from the inclusion of the l_2 term.

In the nematic phase the two P modes are degenerate, as are the two R modes. The least scattering is from the P modes, which follow a temperature dependence [Eq. (17b)] like that of the order parameter [Eq. (11b)]. The Q fluctuations [Eq. (17a)] have the same temperature dependence as the susceptibility [Eq. (12b)], showing that this is the mode that comes closest to ''going critical.'' Somewhat surprisingly, and unlike that of the P and R modes, the fluctuations of the Q mode are not discontinuous through the transition (although the temperature derivative is) even though the transition is first order.

The applicability of these formulas to both the nematic and isotropic phases has already been partially established by the experiments of McClymer and Keyes [13,14], which, in the terminology of the present paper, used zx and xx polarizations to study the scattered intensities. In both cases the isotropic phase could be fit by Eq. (16), as was already known from many previous experiments. Then, using the parameters t and l determined by these isotropic data and *no other adjustable parameters*, they were able to fit the results of the measurements in the nematic phase, which had never been obtained before. For the zx case a fit to Eq. (17c) for the nematic was verified. The scattering for xx polarization geometry, as discussed in Sec. II A, should be given by a sum of Eqs. (17a) and (17b) in the nematic phase, and this was also confirmed.

IV. THE FIELD-INDUCED UNIAXIAL-UNIAXIAL CRITICAL POINT

In the presence of an applied field the isotropic symmetry of the high temperature phase is broken and we have a uniaxial phase, a ''paranematic,'' one might say. For χ_a positive ($h>0$) the Q order parameter component is positive in both the nematic and the paranematic and at sufficiently high field these two like symmetry phases merge at a critical point. The location of this critical point can be found most readily from Eq. (10), by finding the point at which both the first and second derivatives of t with respect to Q vanish. This procedure yields the critical point parameters [7,8] $h=\frac{1}{27}$, $t=\frac{1}{3}$, and $Q=\frac{1}{3}$.

To find the mode fluctuations for arbitrary values of h and t, one must solve Eq. (10) numerically for Q, which is then used to evaluate the coefficients of Eq. (15), and then use equipartition as before. Approximate analytical expressions can be found by expanding about any point, such as the critical point, but in general numerical solutions must be obtained. Results for the critical field $h=\frac{1}{27}$ are illustrated in Fig. 4 and for twice the critical field in Fig. 5.

Since there is no transition whatsoever for h in excess of the critical field, the high- and low-temperature results must somehow join smoothly onto each other. In this manner one could have surmised that when the field is applied the fivefold mode degeneracy of the isotropic phase must split into one single and two twofold modes as we already have in the nematic phase. Furthermore, one thus also expects that in the high-temperature region the field will cause the Q and R branches in Figs. 4 and 5 to curve downward and the P branch to curve upward. In other words, in the high-temperature region the field initially *enhances* the Q and R fluctuations but *diminishes* the P fluctuations. In fact, the Q fluctuations are enhanced to the point that they actually diverge (for $q=0$) at the critical point; the Q mode is the mode that goes critical in this case. If one increases the field to values larger than the critical, the fluctuations eventually decrease in magnitude. Therefore, looking for a maximum in the scattering from the Q or R modes as a function of field would be a good way of locating the critical region.

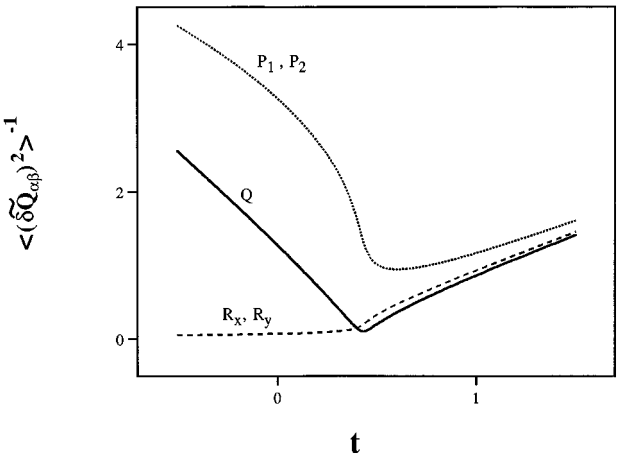

FIG. 5. Inverse of the average square fluctuations of the order parameter components for $q=0$ in the supercritical region above the field-induced nematic-paranematic critical point. Here a reduced field of $h=\frac{2}{27}$, twice the critical field, has been assumed.

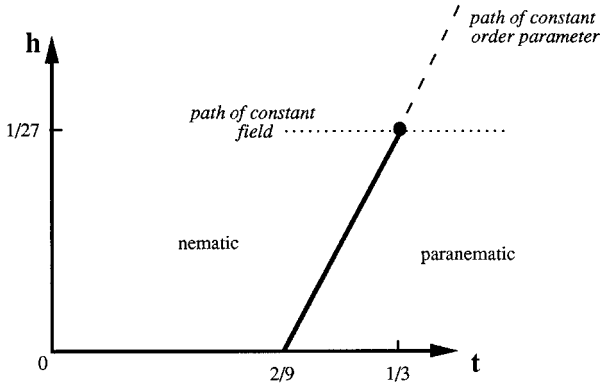

FIG. 6. h-t phase diagram for the nematic-paranematic transition. The solid point represents the field-induced critical point. The dotted line indicates the path assumed for the results shown in Fig. 4, the dashed line the path needed to obtain ''conventional'' critical exponents.

Since this phase transition taking place in the presence of a field is not a symmetry-breaking transition anymore, there are no longer any Goldstone modes. Thus the R fluctuations are now found to be *finite* in the low-temperature phase. This is the well-known quenching of director fluctuations by an external field [1]. As can be seen in the figures, this quenching is not very effective even at the relatively large fields needed to reach the critical region; the director fluctuations in the low-temperature phase remain dominant except for a narrow temperature range just below the critical temperature near where the Q fluctuations diverge. At any given fixed temperature below $t=\frac{2}{9}$, the fluctuations of the Q and P modes are quenched by the field as well, but this is also a rather weak effect.

The functional form of the divergence of the Q fluctuations on the approach to the critical point is particularly interesting. The inset of Fig. 4 reveals that this inverse susceptibility has a cusp at the critical temperature, indicating a critical exponent less than 1. It is a simple matter to expand about the critical point and show that the Q fluctuations in fact diverge like $|\delta t|^{-2/3}$, where δt is the temperature difference from the critical temperature $t=\frac{1}{3}$.

This unusual exponent of $\frac{2}{3}$ is a consequence of the particular path that we have chosen to approach the critical point. It turns out that the van der Waals mean-field theory also predicts this type of divergence for the density fluctuations if one were to approach the liquid-gas critical point along the critical isobar, analogous to the constant h field path we have used here. In both cases the path is oblique to the line of phase transitions that culminate in the critical point and in such cases, according to the geometric picture of Griffiths and Wheeler [20], the susceptibility diverges with the exponent $1-1/\delta$ and *not* the more usual exponent γ. In order to measure a divergence with exponent γ, one has to follow a path of constant order parameter. While it is a relatively simple matter to follow such a path in the liquid-gas case, i.e., an isochore, it is rather impractical to do so in the case of the nematic liquid crystal. We show in Fig. 6 the phase diagram illustrating these two different kinds of paths.

Although $1-1/\delta$ is equal to $\frac{2}{3}$ in the mean-field case where $\delta=3$, it is expected to have a somewhat different value at the paranematic-nematic critical point when one takes fluctuation effects into account. In that case one expects three-dimensional ($d=3$) Ising-like exponents [n, the number of components having diverging fluctuations at this transition, equals 1 since there are no transverse Goldstone modes] and thus $\delta\approx 5$, leading to $1-1/\delta\approx 0.8$, somewhat larger than the mean-field result of $\frac{2}{3}$, but still significantly less than 1. The P and R fluctuations follow cube root dependences about the critical temperature, namely $\langle \delta P_2\rangle^{-1}\approx \frac{10}{9}-8(\delta t)^{1/3}/3^{4/3}$ and $\langle \delta R^2\rangle^{-1}\approx \frac{1}{9}+(\delta t)^{1/3}/3^{4/3}$.

V. THE FIELD-INDUCED UNIAXIAL-BIAXIAL TRANSITION

A. Order parameters and phase diagram

When the coupling constant χ_a is negative ($h<0$) the paranematic induced at higher temperatures by a field along the z direction has a *negative* order parameter Q and is a phase in which the molecules prefer to point *away from* the symmetry direction rather than along it. Upon cooling through the phase transition temperature the molecules spontaneously orient along a new direction perpendicular to the field, which we will shall take to be the x direction. This new ordering is characterized by an additional order parameter P_1 and the nematic liquid crystal is thus biaxial or, perhaps more accurately, ''parabiaxial.'' For weak fields the x axis may be thought of as the ''real'' or primary director and P_1 as the primary order parameter. The z axis is then a secondary director, a direction of slight breaking of the circular symmetry about the x axis. At larger fields, however, where the biaxiality is strong, the distinction between primary and secondary directors is less meaningful.

The nature of the phase transition is greatly altered by having a negative rather than a positive anisotropy. There can no longer be a critical point, since the high- and low-temperature phases now have *different* symmetries, but the transition between these two phases can change from being first order at low fields to second order at high fields. The point where this changeover takes place is a tricritical point and its location can be determined by examining the free-

energy density of Eq. (8) for the case of the biaxial nematic where we have nonzero values for both Q and P_+ order parameters, namely,

$$\mathcal{F}=\tfrac{1}{2}t(Q^2+P_1^2)-\tfrac{1}{3}Q^3+QP_1^2+\tfrac{1}{4}(Q^2+P_1^2)^2-hQ. \tag{18}$$

Minimization of this free-energy density expression with respect to P_1 yields two possibilities.

First, there is the solution where $P_1=0$, which describes the high-temperature side of the transition, that is, the *uniaxial phase*. Subsequent minimization with respect to Q then gives

$$0=tQ-Q^2+Q^3+|h|, \tag{19}$$

which is the same as Eq. (10) except that we have in this case replaced $-h$ by the absolute value of h to remind ourselves that $h<0$. For $h\neq 0$ this is solved numerically for the equilibrium values of Q_0.

Second, Eq. (18), minimized with respect to P_1, also has the solution

$$P_1^2=-t-2Q-Q^2, \tag{20}$$

which describes the low-temperature side of the transition, the *biaxial phase*. Substituting Eq. (20) into Eq. (18) and then minimizing with respect to Q yields a relation that can be solved analytically for Q (from now on we drop the ''o'' subscript from the equilibrium values):

$$Q=-\tfrac{1}{4}-\tfrac{1}{4}\sqrt{1-4(h+t)}. \tag{21}$$

This, in turn, can be used in Eq. (20) to obtain the equilibrium values of P_1:

$$P_1^2=-\frac{3}{4}t+\frac{3}{8}+\frac{h}{4}+\frac{3}{8}\sqrt{1-4(h+t)}. \tag{22}$$

It is then an easy matter to show that the transition becomes second order at large fields [9] and that the coordinates of the tricritical point are given by $h=-\frac{3}{16}$ and $t=\frac{7}{16}$. Furthermore, the line of second-order transitions for fields larger than the tricritical value is given by

$$t=2\sqrt{-\frac{h}{3}}+\frac{h}{3}. \tag{23}$$

The phase diagram is shown schematically in Fig. 7.

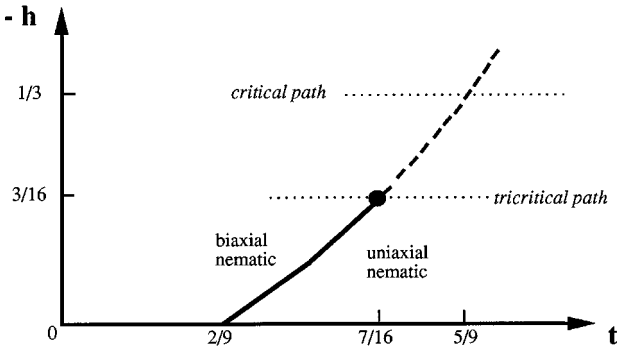

FIG. 7. h-t phase diagram for the field-induced uniaxial-biaxial nematic phase transition. (It is convenient to use $-h$ as the ordinate when $\chi_a<0$.) The heavy dashed line is a line of second-order transitions and the solid line a line of first-order transitions. The solid point represents the tricritical point. The lower and upper dotted lines indicate, respectively, the paths used in obtaining the results of Figs. 8 and 9.

B. Calculation of the Fluctuations

When Q and P_1 are both nonzero and fluctuations are included, Eq. (8) yields

$$\begin{aligned}\mathcal{F}_2=&\tfrac{1}{2}(t-2Q+3Q^2+P_1^2)\,\delta Q^2+2P_1(1+Q)\,\delta Q\,\delta P_1\\&+\tfrac{1}{2}(t+2Q+Q^2+3P_1^2)\,\delta P_1^2+\tfrac{1}{2}(t+2Q+Q^2+P_1^2)\,\delta P_2^2\\&+\tfrac{1}{2}(t-Q-\sqrt{3}P_1+Q^2+P_1^2)\,\delta R_x^2\\&+\tfrac{1}{2}(t-Q+\sqrt{3}P_1+Q^2+P_1^2)\,\delta R_y^2.\end{aligned} \tag{24}$$

The coefficient of the second term, the cross term in δQ and δP_1, is zero in the high-temperature phase where $P_1=0$ and so this term causes no problems there. All five modes are then normal modes and we may use equipartition as before to calculate the fluctuations. The principal difference from before is that the field now induces *negative* values of the Q order parameter and so enhances the scattering from the P fluctuations while diminishing that of the Q fluctuations. The roles of the Q and P order parameters are thus more or less reversed; the P fluctuations eventually go critical while those of Q are quenched by the field at any given temperature. This is shown in Figs. 8 and 9 for two values of the field, the tricritical value $h=-\frac{3}{16}$, and a representative larger negative value $h=-\frac{1}{3}$.

In the low-temperature phase, where the cross term is not zero, δQ and δP_1 are no longer normal modes and we must use an *extended* equipartition theorem to calculate the fluctuations in these quantities. By this we mean that when one has an energy expression with a cross term such as $ax^2+bxy+cy^2$, where x and y are variables and a, b, and c are constants, then straightforward integration gives $\langle x^2\rangle=2ck_BT/(4ac-b^2)$ and a like expression for $\langle y^2\rangle$ with the c and a variables interchanged. In this manner we have

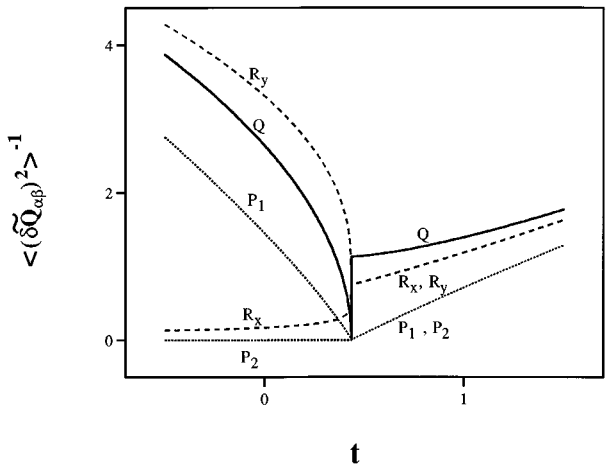

FIG. 8. Inverse of the average square fluctuations of the order parameter components for $q=0$ in the vicinity of the field-induced uniaxial-biaxial tricritical point. The tricritical temperature is $t=\frac{7}{16}$.

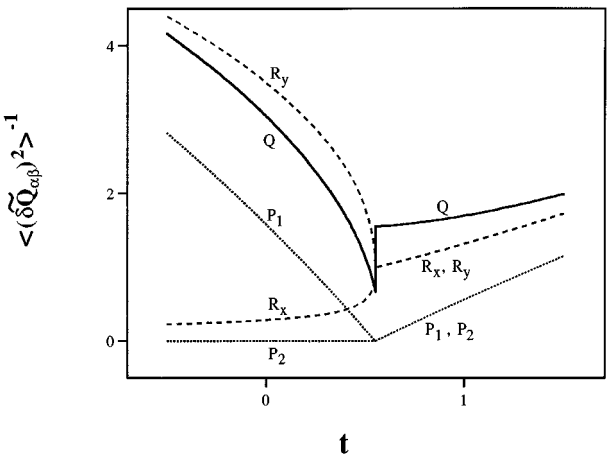

FIG. 9. Inverse of the average square fluctuations of the order parameter components for $q=0$ in the vicinity of a field-induced uniaxial-biaxial critical point. Here a reduced field of $h=-\frac{1}{3}$ is assumed, corresponding to a critical temperature of $t=\frac{5}{9}$.

obtained the results shown in Figs. 8 and 9 for the low-temperature side of the transition. (Note that we could have diagonalized the energy expression to find the particular linear combinations of δQ and δP_1 at each temperature that *are* normal modes, but this would be of little interest to the experimentalist who actually measures the fluctuations in δQ and δP_+ regardless of whether or not they happen to be normal modes.)

C. Discussion of results

1. The tricritical point

We can see from Fig. 8 that P is really the primary ordering, as mentioned earlier. Both P modes become critical as the transition temperature is approached from above and likewise P_1 goes critical as the phase transition is approached from below. P_2 remains critical-like throughout the low-temperature phase, showing that it is a Goldstone mode. By expanding about the tricritical point, the exact manner in which P_1 approaches zero from the low-temperature side of the transition can be deduced. From Eq. (22) we find $P_1^2 \approx 3/4\sqrt{-\delta t}$ in the vicinity of this point, indicating that the order parameter exponent β is $\frac{1}{4}$, as expected for a tricritical point.

The temperature behavior of the Q order parameter is of a different form above and below the tricritical temperature. Below it approaches its tricritical value of $-\frac{1}{4}$ with a square-root dependence: $Q\approx-\frac{1}{4}-\sqrt{-\delta t}/2$, according to Eq. (21); above it varies linearly: $Q\approx-\frac{1}{4}+2\,\delta t/9$, as found from Eq. (19).

The fluctuations in P_1 are given by $\langle \delta P_1^2\rangle^{-1}\approx-16\delta t/3$ below the transition and $\langle \delta P_1^2\rangle^{-1}\approx-4\,\delta t/3$ above. The ratio of these two amplitudes is 4:1, as expected for a tricritical point. The obvious curvature of the P_1 results in Fig. 8 indicates that the domain over which these linear temperature dependences apply is limited to a small region near the tricritical temperature.

The two R modes, degenerate in the high-temperature phase, approach the transition linearly from above: $\langle \delta R_x^2\rangle^{-1}=\langle \delta R_y^2\rangle^{-1}\approx\frac{3}{4}+2\,\delta t/3$. Below the transition this degeneracy is split suddenly and very strongly: $\langle \delta R_x^2\rangle^{-1}\approx\frac{3}{4}-\frac{3}{2}(-\delta t)^{1/4}$ and $\langle \delta R_y^2\rangle^{-1}\approx\frac{3}{4}+\frac{3}{2}(-\delta t)^{1/4}$. These $\frac{1}{4}$ power laws mirror the temperature dependence of the order parameter, which has the same critical exponent.

The behavior of the Q mode is perhaps the most unusual. Even though the transition is continuous at the tricritical point, the fluctuations of this mode are *discontinuous*. In this respect it behaves something like the specific heat at an ordinary second-order mean-field transition. But, unlike that specific-heat behavior, which is just a simple discontinuity, the Q fluctuations *diverge* on the low-temperature side of the transition. Specifically, we find a square-root singularity $\langle \delta Q^2\rangle^{-1}\approx 4\sqrt{-\delta t}$ below the transition and $\langle \delta Q^2\rangle^{-1}\approx\frac{9}{8}+2\,\delta t/9$, a linear relation, above.

One of the chief characteristics of a tricritical point is that fluctuation effects do not cause significant departures from the predictions of mean-field theory. Therefore, the critical exponents, amplitude ratios, and other critical features we have calculated here are expected to be the actual behaviors that will be observed experimentally for this type of tricritical point. The correctness of the mean-field approach at the tricritical point of various systems with vector order parameters has already been established. It will be interesting to see whether this approach is equally valid for this five-component tensor order parameter, particularly when some of the predicted effects, such as the Q fluctuation behavior, are so unconventional.

2. The line of critical points

For fields greater than the tricritical value the phase boundary is a line of second-order transitions. Approaching any point on this boundary is the same as approaching a critical point. In a region close to the tricritical point there will be a competition between the two types of critical behavior and a ''crossover'' from the tricritical to the critical behavior. We consider a critical point sufficiently far from the tricritical point that these crossover effects are not observed in the temperature range of interest. Specifically, we calculate the fluctuation effects for a field of $h=-\frac{1}{3}$, which has a critical temperature of $t=\frac{5}{9}$ according to Eq. (23). The path of temperature variation is indicated by the upper dotted line in Fig. 7. The behavior along this path should be representative of all temperature scans sufficiently far above the tricritical point.

Expanding about the critical point having the above parameters, we find that the primary order parameter varies as $P_1^2\approx-3\,\delta t$, indicating that the exponent β is now $\frac{1}{2}$, as expected for a mean-field critical point. The temperature dependence of the Q order parameter is $Q=-\frac{1}{3}-3\,\delta t/2$ below the transition and $Q\approx-\frac{1}{3}+3\delta t/14$ above, a linear variation in both cases.

The behavior of the fluctuations, shown in Fig. 9, is also quite different from what was found for the tricritical point. The temperature variation of the P_1 fluctuations, those of the primary order parameter, are as one would expect the susceptibility to behave at a mean-field second-order transition. There is a linear dependence on both sides: $\langle \delta P_1^2\rangle^{-1}\approx-18\delta t/7$ below the transition and $\langle \delta P_1^2\rangle^{-1}\approx 9\,\delta t/7$ above, and hence a 2:1 amplitude ratio as also expected. The P_2 mode, of course, continues to be a Goldstone mode below the transition.

The two R modes again approach the transition linearly from above, this time as $\langle \delta R_x^2 \rangle^{-1} = \langle \delta R_y^2 \rangle^{-1} \approx 1 + 9\,\delta t/14$. Below the transition the two modes now follow square-root singularities: $\langle \delta R_x^2 \rangle^{-1} \approx 1 - 3(-\delta t)^{1/2}$ and $\langle \delta R_y^2 \rangle^{-1} \approx 1 + 3(-\delta t)^{1/2}$. These power laws once again mirror the temperature dependence of the order parameter. It appears, therefore, that the measurement of the R mode fluctuations is evidently a good independent way to study the order parameter variation for both the critical and the tricritical situations.

The Q mode fluctuations are again discontinuous at the transition, in spite of the otherwise continuous nature of the transition, but now there is no singularity on the low-temperature side. Specifically, we find $\langle \delta Q^2 \rangle^{-1} \approx \frac{2}{3} - 12\,\delta t$ below the transition and $\langle \delta Q^2 \rangle^{-1} \approx \frac{14}{9} + \delta t/7$ above. The tricritical point is therefore the only point in the entire h-t space where the Q mode fluctuations diverge (and then only on the low-temperature side). Measurement of these Q fluctuations then should be a good way to experimentally search for the tricritical point.

VI. THE SPONTANEOUS (ZERO-FIELD) UNIAXIAL-BIAXIAL TRANSITION

A. Free energy and calculation of order parameters

In the absence of any applied field at all, a uniaxial nematic liquid crystal may condense into a biaxial nematic if the temperature is lowered far enough [2]. To account for such a phenomenon within the context of Landau–de Gennes theory it is necessary to carry out the free-energy expansion to sixth order. That is, to the expression of Eq. (4) one adds the fifth- and two sixth-order terms:

$$\mathcal{F}_{5+6} \equiv D(Q_{\alpha\beta}Q_{\beta\alpha})(Q_{\sigma\mu}Q_{\mu\nu}Q_{\nu\sigma}) + E(Q_{\alpha\beta}Q_{\beta\gamma}Q_{\gamma\alpha})^2 + E'(Q_{\alpha\beta}Q_{\beta\alpha})^3. \tag{25}$$

The fifth-order D term gives an asymmetry between positive and negative values of the order parameter Q, as is needed to reproduce the type of skewed phase diagram seen in some experiments. But this term does not give rise to biaxiality and, to the contrary, tends to suppress it as likewise does the E' term [1,16]. To simplify the following discussion we will reduce the number of free parameters by setting these D and E' coefficients equal to zero while retaining the E term, all that is really necessary to obtain a biaxial phase. Performing the same scaling of variables as we did in obtaining Eq. (5), we obtain:

$$\mathcal{F} = \tfrac{1}{2} t Q_{\alpha\beta}Q_{\beta\alpha} - \sqrt{\tfrac{2}{3}} Q_{\alpha\beta}Q_{\beta\gamma}Q_{\gamma\alpha} + \tfrac{1}{4}(Q_{\alpha\beta}Q_{\beta\alpha})^2 + e(Q_{\alpha\beta}Q_{\beta\gamma}Q_{\gamma\alpha})^2. \tag{26}$$

In the above we have omitted the gradient and external field terms, not of interest to us at the moment, and have defined a new dimensionless variable $e \equiv EB^2/C^3$.

Now, as in Sec. V, we look for the equilibrium minima of Eq. (26) that have only the Q and P_1 order parameters nonzero. That is, we look for the minima of

$$\mathcal{F} = \tfrac{1}{2} t(Q^2 + P_1^2) - \tfrac{1}{3} Q^3 + Q P_1^2 + \tfrac{1}{4}(Q^2 + P_1^2)^2 + \tfrac{3}{2} e(\tfrac{1}{3} Q^3 - Q P_1^2)^2. \tag{27}$$

Minimizing this equation with respect to P_1 yields

$$P_1(t + 2Q + Q^2 - 2eQ^4) + P_1^3(1 + 6eQ^2) = 0, \tag{28}$$

which may be solved for P_1 to be substituted back into Eq. (27), which is, in turn, minimized with respect to Q. In this manner we (numerically) find the equilibrium values of Q and P_1 for both the uniaxial and the biaxial phases. The uniaxial solution to Eq. (28) i.e., $P_1 = 0$, becomes unstable when the expression in the first set of parentheses ceases to be positive; this signals the (second-order) transition to the biaxial phase

$$t + 2Q + Q^2 - 2eQ^4 = 0. \tag{29}$$

Also, within the uniaxial phase, Q must satisfy the equation

$$t - Q + Q^2 + eQ^4 = 0. \tag{30}$$

Putting these last two equations together tells us that the uniaxial-biaxial transition takes place when the reduced temperature t and the reduced sixth-order coefficient e are related by $t = -e^{-2/3}$, and at this transition the order parameter Q will be given by $Q = \sqrt{-t}$.

B. Calculation of the fluctuations

Now, as we have done to obtain Eq. (24), we expand about the local minimum to obtain the harmonic free energy for the fluctuations $\delta Q_{\alpha\beta}$. The results are similar to those of Eq. (24), but more involved because of the sixth-order term:

$$\begin{aligned}
\mathcal{F}_2 = {} & \tfrac{1}{2}(t - 2Q + 3Q^2 + P_1^2 + 5eQ^4 + 3eP_1^4 - 12eQ^2P_1^2)\,\delta Q^2 \\
& + 2P_1(1 + Q + 6eQP_1^2 - 4eQ^3)\,\delta Q\,\delta P_1 + \tfrac{1}{2}(t + 2Q \\
& + Q^2 + 3P_1^2 + 18eQ^2P_1^2 - 2eQ^4)\,\delta P_1^2 + \tfrac{1}{2}(t + 2Q + Q^2 \\
& + P_1^2 + 6eQ^2P_1^2 - 2eQ^4)\,\delta P_2^2 + \tfrac{1}{2}(t - Q - \sqrt{3}P_1 + Q^2 \\
& + P_1^2 + eQ^4 + \sqrt{3}eQ^3P_1 - 3eQ^2P_1^2 - 3\sqrt{3}ePQ_1^3)\,\delta R_x^2 \\
& + \tfrac{1}{2}(t - Q + \sqrt{3}P_1 + Q^2 + P_1^2 + eQ^4 - \sqrt{3}eQ^3P_1 \\
& - 3eQ^2P_1^2 + 3\sqrt{3}eQP_1^3)\,\delta R_y^2.
\end{aligned} \tag{31}$$

Once again there is a $\delta Q\,\delta P_1$ cross term and so we must use the extended equipartition theorem, as we did in Sec. V B, to evaluate the fluctuations of Q and P_1 in the biaxial phase. Since the equations for the equilibrium values are now of higher algebraic order, almost all results must now be obtained numerically.

C. Discussion of results

The fluctuations are now not only a function of the reduced temperature t, but also of e, the reduced sixth-order coefficient. Different values of e produce qualitatively similar results for the fluctuations. Therefore, we first present representative results calculated for $e = 1$ and then briefly comment on some of the effects of changing e.

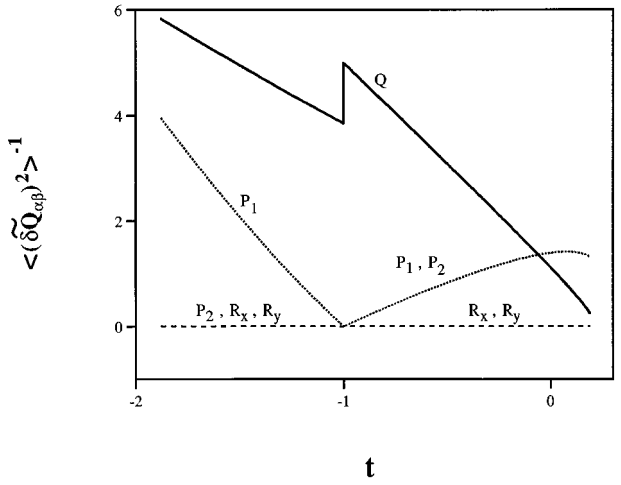

FIG. 10. Inverse of the average square fluctuations of the order parameter components for $q=0$ in the vicinity of the spontaneous (zero-field) uniaxial-biaxial transition. Here a reduced sixth-order coefficient of $e=1$ has been assumed, resulting in a uniaxial-biaxial transition temperature of $t=-1$.

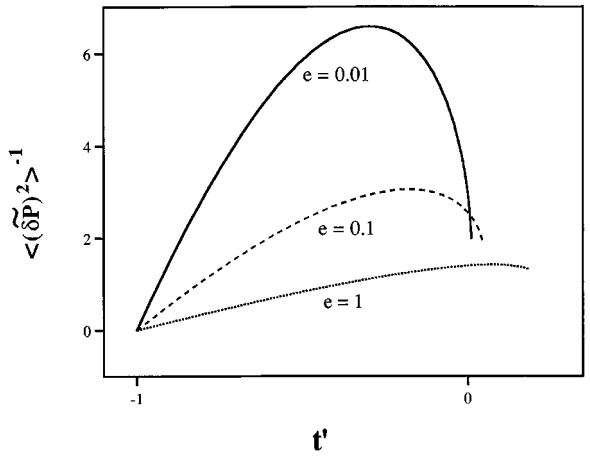

FIG. 11. Inverse of the average square fluctuations of the P order parameter components for $q=0$ in the vicinity of the spontaneous (zero-field) uniaxial-biaxial transition. Three different reduced sixth-order coefficients of e have been assumed, each corresponding to the same reduced uniaxial-biaxial transition temperature t', defined as $t'\equiv t/e^{-2/3}$.

The five inverse susceptibilities in both the uniaxial and biaxial phases for $e=1$ are plotted in Fig. 10. We do not include results for the isotropic phase, since they are identical to those of Fig. 3 except for the fact that the transition temperature is shifted slightly downward when the sixth-order term is included. Note that uniaxial results are also similar to those of Fig. 3 very near the transition to the isotropic phase, but then deviate substantially as the temperature is lowered toward the transition to the biaxial phase.

From the relation for the phase boundary $t=-e^{-2/3}$, given in Sec. V, we see that the uniaxial-biaxial transition takes place at a reduced temperature $t=-1$ when the reduced sixth-order coefficient $e=1$. Below this temperature P_2 becomes a new Goldstone mode. Detection of the fluctuations of this third Goldstone mode by light scattering provides another independent way in which one can prove the existence of a purported biaxial nematic phase.

The P_1 fluctuations are found to diverge linearly on both sides of the transition, but with an amplitude that is twice as large on the high-temperature side as on the low, which is standard behavior for a second-order, mean-field phase transition. Since it is the two-component set of P parameters that order, it is expected on theoretical grounds that this transition should fall into the $n=2$, $d=3$ universality class. Consequently, if one can get close enough to the transition to experience strong fluctuation effects, one should measure exponents $\gamma=\gamma'\approx 1.3$ for the divergence of the fluctuations rather than the linear mean-field behavior. The amplitude ratio would likewise be modified from its mean-field result by the critical fluctuations.

The Q fluctuations are here again discontinuous at the transition in spite of its otherwise continuous nature. In this case, however, there is no hint of any singular behavior on either side of the transition as there was for the field-induced uniaxial-biaxial transition at the tricritical point in Sec. V.

Perhaps the most interesting of all is the behavior of the P fluctuations in the region between the two transitions. The inverse susceptibility $\langle \delta P^2 \rangle^{-1}$ rises on cooling from the isotropic-nematic transition, reaches a maximum, and then falls as it approaches the uniaxial-biaxial transition, where it goes to zero. This general trend could have been anticipated, but what is surprising is that the maximum is so far removed from the uniaxial-biaxial transition. The appearance of such a maximum allows one to predict that a biaxial phase probably lies at lower temperatures while one is still far removed from it. To some extent this feature is dependent upon the specific value of e that we have chosen. If e is made very small, the maximum moves downward in temperature but no farther than the midpoint between the two phase transitions. We show this trend in Fig. 11, where we have plotted $\langle \delta P^2 \rangle^{-1}$ versus reduced temperature $t'\equiv t/e^{-2/3}$ for three widely different values of e. We conclude that if there is a tendency to form a biaxial phase at a lower temperature, even lower than one might be able to reach before some other phase forms instead, one should be able to detect this incipient transition without having to go more than halfway toward it.

The occurrence of thermodynamically stable biaxial nematic phases is rare. There are numerous examples of biaxial shaped molecules, and of mixtures of rod and plate shaped molecules, having uniaxial nematic phases, that might be expected to form a biaxial nematics upon cooling but do not. It would be useful to measure the temperature dependence of the biaxial fluctuations in the nematic phases of some of these systems to see if the light scattering reveals any tendency to form a lower temperature biaxial phase. The nematic–smectic-C transition is another system where such studies could prove enlightening, particularly in the vicinity of the nematic–smectic-A–smectic-C multicritical point where a biaxial nematic has been predicted [21] but never seen.

VII. THE LANDAU MULTICRITICAL POINT

The appearance of a field-free uniaxial-biaxial nematic phase transition, of the type discussed in the preceding section, is usually linked to the presence of a nearby Landau point. This point is a special type of multicritical point, dif-

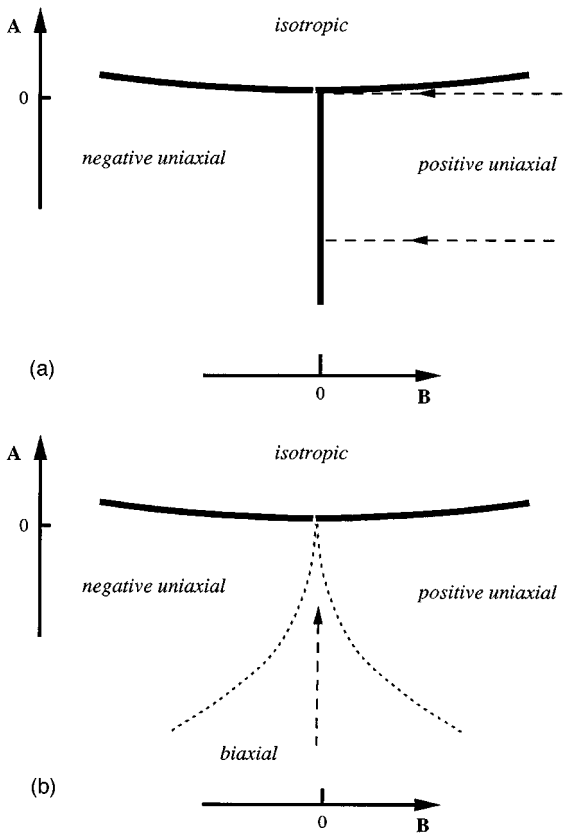

FIG. 12. Schematic phase diagrams in the vicinity of the Landau point when the sixth-order coefficient (a) $E \leqslant 0$ and (b) $E > 0$. Solid lines mark first-order transitions, dotted lines second-order transitions, and the dashed lines with arrows indicate paths discussed in the text.

ferent from the other types of critical points discussed so far, whose properties will now be discussed separately.

A. Free energy and phase diagrams

The Landau point is defined by the simultaneous vanishing of the quadratic coefficient A and the cubic coefficient B in the free-energy expression of Eq. (4). It is in the vicinity of this point that one is most likely to find a biaxial nematic phase. Two different types of phases diagrams are possible. One has a biaxial ''wedge'' sandwiched between two uniaxial phases of opposite signs, while the other has just the two uniaxial phases separated by a line of first-order transitions [1,16]. Both types of phase diagrams have been found experimentally [4]. Whether or not the biaxial wedge appears depends upon the values of the fifth- and sixth-order coefficients. In the specific model we have been considering, where the coefficients D and E' are assumed to be zero, the biaxial phase appears when $E > 0$, while the phase diagram having no biaxial region is found for $E \leqslant 0$. The following discussion will be restricted to this simplified model. The phase diagrams, using A and B as the independent variables, are illustrated schematically in Fig. 12.

Most of the phase transitions shown in these two phase diagrams, such as the isotropic-uniaxial and uniaxial-biaxial transitions, have already been discussed in previous sections. Therefore, in this section we consider only those transitions that are new, such as the uniaxial-uniaxial transitions appearing in Fig. 12(a) and those transitions involving an approach to the Landau point itself, one of which is indicated by the dashed line in Fig. 12(b).

B. Calculation of the fluctuations and discussion of results

All of these special types of transitions associated with the Landau point have either B approaching zero or else B held at zero while A approaches zero. Therefore, if we are to use the results of the previous sections, such as Eq. (31), for example, to calculate the fluctuations, we must do so with care since the variable B has been used as a scaling variable as in $t \equiv AC/B^2$, etc. It would be better for the present purposes to transpose the previously obtained results using a scaled temperature $\hat{t} \equiv A/C$ (as is usually done when there is no cubic term in the free energy). We also will find it convenient to define a scaled cubic coefficient $\hat{b} \equiv B/C$ and a scaled sixth-order coefficient $\hat{e} \equiv E/C$.

Because of the complexity of the equations when the sixth-order term is retained, only numerical solutions for the fluctuations can be obtained in general. In order to gain insight into the nature of these solutions, it is useful wherever possible to consider limiting cases that admit of analytical solutions. These special cases will be the focus of much of the following discussion.

1. $\hat{e} = 0$: The uniaxial-uniaxial transition and the approach to the Landau point

With the above changes in notation implemented, we have for the *isotropic* phase, in lieu of Eq. (16),

$$\langle \widetilde{\delta Q}^2 \rangle = \langle \widetilde{\delta P}_1^2 \rangle = \langle \widetilde{\delta P}_2^2 \rangle = \langle \widetilde{\delta R}_x^2 \rangle = \langle \widetilde{\delta R}_y^2 \rangle = \frac{k_B T}{C} \frac{1}{\hat{t}}. \tag{32}$$

Likewise, for the *nematic* side of the transition, in place of Eqs. (17) we obtain

$$\langle \widetilde{\delta Q}^2 \rangle = \frac{k_B T}{C} \frac{2}{\hat{b}^2 - 4\hat{t} + \hat{b}\sqrt{\hat{b}^2 - 4\hat{t}}}, \tag{33a}$$

$$\langle \widetilde{\delta P}_1^2 \rangle = \langle \widetilde{\delta P}_2^2 \rangle = \frac{k_B T}{C} \frac{\frac{2}{3}}{\hat{b}^2 + \hat{b}\sqrt{\hat{b}^2 - 4\hat{t}}}. \tag{33b}$$

All of these results are quoted for the $q = 0$ limit, where the R fluctuations within the nematic phase diverge and are therefore not given.

In the new notation the phase boundary between the nematic and isotropic phase, previously given by $t = \frac{2}{9}$, now becomes $\hat{t} = 2\hat{b}^2/9$. This parabolic relation between these two reduced variables for the phase boundary leads to a doubling of the critical exponents if the Landau point is approached by varying $\hat{b}$ rather than $\hat{t}$, as along the path indicated by the upper dashed line in Fig. 12(a). Thus, from Eqs. (33) we see that both the Q and P fluctuations within the nematic phases vary as $\hat{b}^{-2}$ if $\hat{t}$ is held at zero. This divergence with an exponent of 2 is a geometrical effect [20] caused by approaching the isotropic-nematic phase transition boundary tangentially rather than obliquely. If, however, $\hat{b}$ is held at

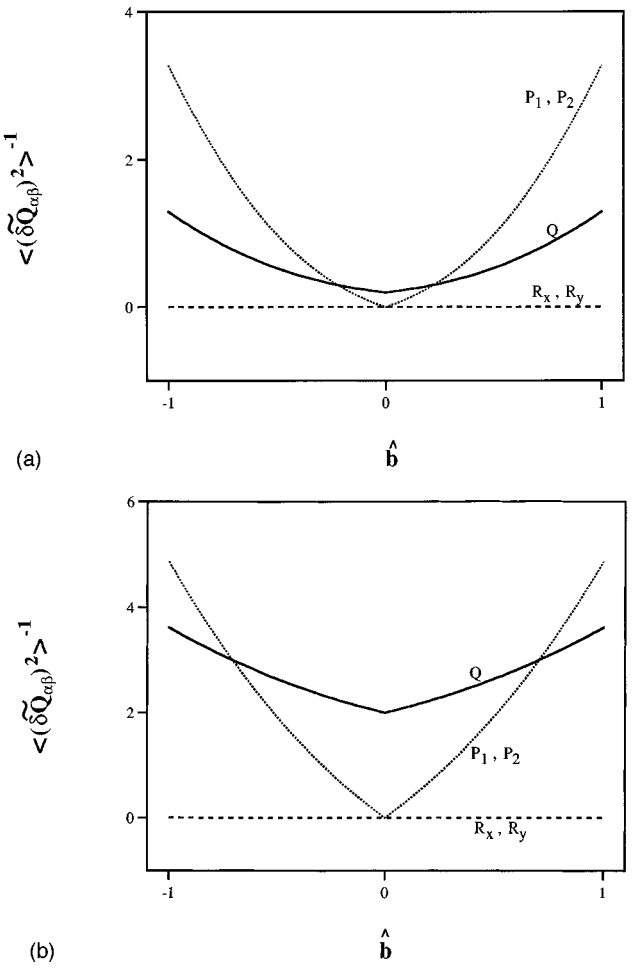

FIG. 13. Inverse of the average square fluctuations of the order parameter components for $q=0$ in the vicinity of the first-order uniaxial-uniaxial phase transition corresponding to the lower dashed line of Fig. 12(a). Reduced temperatures of (a) $\hat{t}=-0.1$ and (b) $\hat{t}=-1$ have been assumed.

zero and $\hat{t}$ is varied, we see from Eqs. (32) and (33a) that the Q fluctuations behave normally with linear divergences and a 2:1 amplitude ratio as expected at an ordinary second-order phase transition. The effects of varying $\hat{b}$, although interesting, are largely of academic interest, since it will probably not be easy to perform this variation experimentally, at least not in a continuous fashion.

When $\hat{b}$ and $\hat{t}$ are both nonzero, a crossover between the exponents of 2 and 1 is seen as $\hat{b}$ is varied. This phenomenon is illustrated in Fig. 13, where we show the inverses of the Q, P, and R fluctuations as a function of $\hat{b}$. When $\hat{t}$ is small and we are close to the Landau point, as in Fig. 13(a), the quadratic behavior dominates. When $\hat{t}$ is larger and we are farther from the Landau point, as in Fig. 13(b), the linear dependence prevails over most of the region of interest.

It is a curious feature of this model that the P fluctuations diverge at $\hat{b}=0$ even though the transition between the two uniaxial phases is first order. This exceptional behavior can be understood by realizing that $\hat{e}=0$ is a special case bordering two rather different behaviors. If $\hat{e}$ were just slightly positive, rather than zero, we would be passing through a second-order uniaxial-biaxial transition, as in Fig. 12(b), as $\hat{b}$ goes to zero. This incipient second-order behavior is the origin of the divergence of the P fluctuations; it goes away when $\hat{e}$ is negative, as discussed below.

2. $\hat{e}<0$: The uniaxial-uniaxial transition and the approach to the Landau point

Although analytical solutions are not feasible in this case, semiquantitative insights can be gained by considering the addition of the sixth-order term as a perturbation to the above case of $\hat{e}=0$. This point of view is certainly valid near the Landau point where the Q and P parameters are small. The modifications to the Q fluctuations will be slight, as long as $\hat{e}$ is not too largely negative, and the Q results will still look very much like those shown in Fig. 13. The P_1 fluctuations, however, are changed substantially, particularly in the vicinity of the uniaxial-uniaxial transition. We can see by reference to Eq. (31), for example, that the coefficient of the δP_1^2 term in the free energy will now have an extra $\hat{e}Q^4$ term. Near the uniaxial-uniaxial transition ($\hat{b}=0$) we have $Q^4 \sim A/C \sim \hat{t}^2$ (as long as $\hat{e}$ is not too big) and so the net result is that the P_1 fluctuations, rather than diverging at the first-order transition between the two uniaxial phases, will now be given by $\langle \delta P_1^2 \rangle \approx -k_B T/(3C\hat{e}\hat{t}^2)$ and are finite. As the Landau point is approached, however, they once again diverge and do so with an exponent of 2 if temperature is the variable. The P_2 fluctuations continue to diverge at the uniaxial-uniaxial phase boundary, much as they did in Fig. 13.

3. $\hat{e}>0$: The approach to the Landau point through the biaxial nematic region

Now we will consider the path indicated by the dashed line in Fig. 12(b) that follows $B=0$, $\hat{t}\to 0$ with $\hat{e}>0$, so that there is a biaxial nematic region. It turns out that analytical solutions are possible in this case (with the cubic term absent, the quartic equation we must solve for Q is actually a quadratic equation for Q^2). We now obtain

$$\langle \widetilde{\delta Q}^2 \rangle = \frac{k_B T}{C} \frac{-2+9\hat{e}\hat{t}}{24\hat{e}\hat{t}^2} \xrightarrow[\hat{e},\hat{t}\to 0]{} \frac{k_B T}{C} \frac{-1}{12\hat{e}\hat{t}^2}, \tag{34a}$$

$$\langle \widetilde{\delta P}_1^2 \rangle = \frac{k_B T}{C} \frac{-2+\hat{e}\hat{t}}{4\hat{e}\hat{t}^2} \xrightarrow[\hat{e},\hat{t}\to 0]{} \frac{k_B T}{C} \frac{-1}{2\hat{e}\hat{t}^2}. \tag{34b}$$

In this biaxial phase the P_2 as well as the R_x and R_y modes have diverging fluctuations. An exponent of 2 is found for the temperature divergence of the Q and P_1 fluctuations as the Landau point is neared. This result once again has a geometrical cause: the biaxial-uniaxial boundary is approached tangentially along this path, as may be seen in Fig. 12(b). The $\hat{e}$ divergence has an exponent of 1 because the biaxial-uniaxial boundaries approach a point on the dashed line obliquely with $\hat{e}\to 0$ as the biaxial wedge squeezes in on this line from the two sides.

Renormalization group calculations have been carried out for the vicinity of the Landau point with $\hat{e}=0$ and it has been found that when fluctuation effects are important the critical exponents should be those appropriate to an $n=5$, $d=3$ system [22]. This result makes sense since, as we saw in Sec. VII B 1, the Q mode goes critical at the Landau point with

all four other modes behaving like Goldstone modes. However, as already noted, the case of $\hat{e}=0$ is special and somewhat pathological. The situations with $\hat{e}>0$ and $\hat{e}<0$ are somewhat different in that two modes, Q and P_1 become critical with the other three modes having diverging fluctuations. It is not known at this time what effects, if any, this distinction might have on the predictions for the fluctuation dominated critical behavior when $\hat{e}\neq 0$.

VIII. SUMMARY AND CONCLUSIONS

We have calculated the fluctuations of all five components of the orientational order parameter of a nematic liquid crystal in a wide variety of circumstances involving several types of critical and multicritical points. The predicted behaviors have been more varied and interesting than one might have imagined at the outset, particularly if one is used to thinking of fluctuations as consisting of just director modes. The study of liquid-crystal phase transitions using a variety of polarization geometries designed to probe the behaviors of all five order parameter fluctuations can be a very useful way of studying the complex critical phenomena associated with these systems. We have in mind here not only the orientational phase transitions discussed in this paper, but also transitions involving positional ordering where the coupling between the smectic and the (tensor) nematic order parameters has the potential to provide light-scattering results more interesting and informative than has previously been realized. The extension of these methods to smectic systems is an area we hope to report on in the near future.

The inclusion of chirality into these discussions is another obvious area for further studies. But the study of the blue phases has taught us, among other things, that the seemingly trivial step of removing inversion symmetry can in fact lead to a whole host of new phenomena and complexities. We do not, therefore, expect the extrapolation of these methods to chiral cases to be a simple one, but we anticipate that it will be rewarded with a richness of new and interesting results.

The Landau–de Gennes free-energy expansion that has formed the basis of our analyses permits a self-consistent check of its applicability: the Ginsburg criterion. Once the spectrum of fluctuations has been determined, as it has here, it is relatively straightforward (although possibly quite involved) to assess the importance of higher-order terms that would invalidate the harmonic approximation used in the mean-field approach. In the interests of time and space, we have elected not to do this analysis, but this too could be a profitable area for future studies.

[1] P. G. de Gennes and J. Prost, *The Physics of Liquid Crystals*, 2nd ed. (Oxford University Press, Oxford, 1993).
[2] M. J. Freiser, Phys. Rev. Lett. **29**, 1041 (1970).
[3] R. Alben, Phys. Rev. Lett. **30**, 778 (1973); J. Chem. Phys. **59**, 4299 (1973).
[4] L. Yu and A. Saupe, Phys. Rev. Lett. **45**, 1000 (1980).
[5] J. Hanus, Phys. Rev. **178**, 420 (1969).
[6] P. J. Wojtowicz and P. Sheng, Phys. Lett. **48A**, 235 (1974).
[7] P. H. Keyes, Phys. Lett. **67A**, 132 (1978).
[8] R. M. Hornreich, Phys. Lett. **109A**, 232 (1985).
[9] C. Fan and M. J. Stephen, Phys. Rev. Lett. **25**, 500 (1970).
[10] A. J. Nicastro and P. H. Keyes, Phys. Rev. A **30**, 3156 (1984).
[11] I. Lelidis and G. Durand, Phys. Rev. E **48**, 3822 (1993).
[12] J. Tang and S. Fraden, Phys. Rev. Lett. **71**, 3509 (1993).
[13] J. P. McClymer and P. H. Keyes, Phys. Rev. A **42**, 4764 (1990).
[14] J. P. McClymer and P. H. Keyes, Phys. Rev. E **48**, 2838 (1993).
[15] P. G. de Gennes, Mol. Cryst. Liq. Cryst. **12**, 193 (1971).
[16] E. F. Gramsbergen, L. Longa, and W. H. de Jeu, Phys. Rep. **135**, 197 (1986).
[17] This is the same decomposition as that of Ref. [16], but with a different notation.
[18] R. L. Stratonovich, Zh. Éksp. Teor. Fiz. **70**, 1290 (1976) [Sov. Phys. JETP **43**, 672 (1976)]; V. L. Pokrovskii and E. I. Kats, *ibid*. **73**, 774 (1977) [*ibid*. **46**, 405 (1977)].
[19] T. W. Stinson, J. D. Litster, and N. A. Clark, J. Phys. (Paris) Colloq. **33**, C1-69 (1972).
[20] R. B. Griffiths and J. C. Wheeler, Phys. Rev. A **2**, 1047 (1970).
[21] G. Grinstein and J. Toner, Phys. Rev. Lett. **51**, 2386 (1983).
[22] R. G. Priest and T. C. Lubensky, Phys. Rev. B **13**, 4159 (1976).